

# DESIGN, CONSTRUCTION, and FIELD MAPPING of the HISTRAP PROTOTYPE DIPOLE

B.A. Tatum, D.T. Dowling, R.S. Lord, S.W. Mosko, and D.K. Olsen

Oak Ridge National Laboratory\*, Oak Ridge, TN 37831-6368

## Abstract

HISTRAP is a proposed 2.67 T-m synchrotron-cooler-storage ring having eight 45°, C-design dipole magnets. A prototype dipole has been designed, fabricated, and mapped. The magnet design utilizes curved and angled coil ends to compensate for end effects in the field. Construction of the prototype dipole has been completed by the FNAL magnet factory. The magnetic field has been mapped using a Hall-effect probe affixed to a newly constructed, PC-based, horizontal positioning system. Results of the field mapping are presented.

## Introduction

HISTRAP, Heavy Ion Storage Ring for Atomic Physics, is a proposed synchrotron-cooler-storage ring optimized for advanced atomic physics research<sup>1</sup>. The ring is 46.8 m in circumference and has a maximum magnetic rigidity of 2.67 T-m. In addition to the prototype dipole magnet discussed here, a prototype RF cavity<sup>2</sup> and a vacuum test stand<sup>3</sup> have been built and tested. The most critical aspect of HISTRAP is a laminated pulsed magnet system consisting of 8 dipoles, 12 quadrupoles, 16 sextupoles, and numerous corrector elements positioned around the ring as shown in Fig. 1.

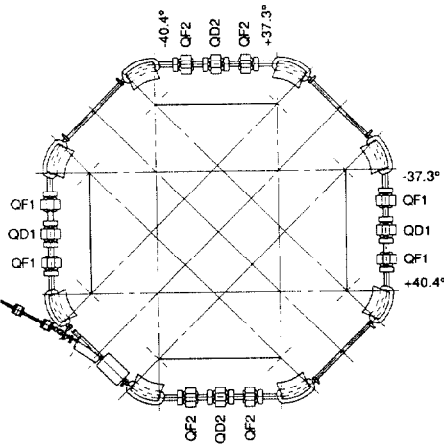


Figure 1: The HISTRAP Lattice

The dipoles require special consideration for several reasons: 1) Their short path length, 131 cm, results in a 3-D geometry with complicated end effects; 2) a large gap, 7 cm, is needed to contain bake-out insulation necessitated by ultra-high vacuum requirements; 3) the radius of curvature is small, 1.67 m, producing a large sagitta which mandates a curved geometry; 4) they must exhibit good field quality from 0.06 to 1.6 T with a 12 cm good field width; and 5) they must be C-shaped to permit merged laser beam studies. To address these concerns, a prototype dipole has been designed, fabricated, and measured.

## Dipole Design

The eight dipoles are conventional, laminated, C-design magnets. Each weighs 12.25 tons including coils, has a 123 cm long yoke, a 12.8-cm sagitta, and parallel ends giving 22.5° beam entrance and exit angles. Lamination cross-sections are 110 cm high by

101 cm wide and the shims and Rogowski roll-off are essentially scaled from the FNAL designed and measured Loma Linda synchrotron dipoles<sup>4</sup>. The Rogowski end cuts also follow standard FNAL practice. Figure 2 shows relative deviations from a pure dipole field as a function of horizontal distance from the central trajectory as calculated by the 3-D magnet code TOSCA.

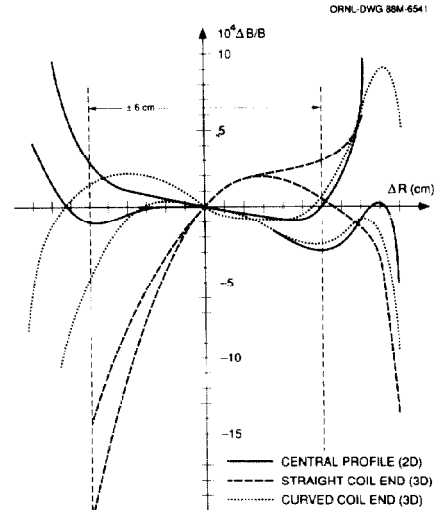


Figure 2: Calculated Field Profiles

The upper curve of each type in Fig. 2 is the result at 0.8 T and the corresponding lower curve is the high-field result at 1.6 T. The solid curves are the field profiles in the center of the dipole, excluding end effects, and are identical to results from the 2-D magnet code POISSON. The permeability drop at high field causes the two curves to separate by about  $4 \times 10^{-4}$  at  $\pm 6$  cm, the horizontal good-field requirement. Equal inside and outside shims give a small quadrupole component to the field profile. The dashed and dotted curves show calculated 3-D TOSCA results, including end effects, obtained by integrating along the ion trajectories through the dipole. The dashed curves show the integrated profiles with straight coil ends parallel to the yoke end. The end effects are large and produce appreciable quadrupole and sextupole components. These components were significantly reduced by curving and angling the coil ends, as shown in Fig. 3.

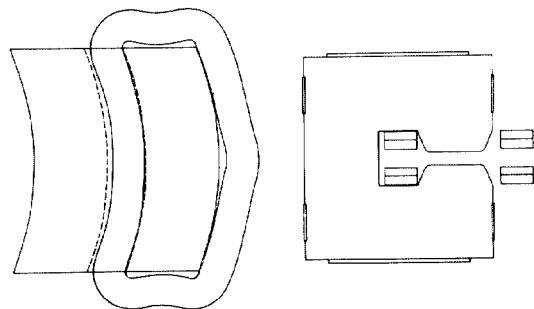


Figure 3: Curved and Angled Coil Ends

The angle of the coil end with respect to the yoke adjusts the integrated quadrupole component, and the

\* Operated by Martin Marietta Energy Systems, Inc. under contract DE-AC05-84OR21400 with the U.S. Department of Energy.

The submitted manuscript has been authored by a contractor of the U.S. Government under contract No. DE-AC05-84OR21400. Accordingly, the U.S. Government retains a nonexclusive, royalty-free license to publish or reproduce the published form of this contribution, or allow others to do so, for U.S. Government purposes.

curvature adjusts the integrated sextupole component. These parameters were optimized to give the calculated field profiles shown as the dotted lines in Fig. 2. This technique corrects most of the integrated field deviations where they occur at the dipole ends.

### Dipole Fabrication

Using this design, a prototype dipole magnet was constructed by FNAL with yoke design and assembly similar to that used for the IUCF dipoles<sup>5</sup>. The yoke was fabricated from laminations punched from 16-gauge SAE 1004-1006 cold-rolled sheet steel purchased from Inland Steel. This steel is phosphate coated to provide electrical insulation between laminations and has a measured permeability of 182 at 100 Oersteds. In order to eliminate dimensional problems induced by the stress in the steel, the laminations were punched with a two-stage die. Sample laminations were dimensionally checked with a Cordax coordinate measuring machine. The pole tips are flat and parallel to within 0.025 mm.

The laminations were washed to improve adhesion, coated with a thin layer of epoxy, and then stacked in an assembly fixture. This fixture was used to stack both the yoke and end assemblies, which consist of removable 7.62 cm-thick end packs bolted to 2.54 cm-thick back packs which were machined with the designed Rogowski contours. The laminations were stacked between these fabricated end assemblies with the gap facing down and centered about a vertical spacer projecting into the gap. Two rails determined the curvature of the magnet yoke. The yoke was then compressed to the proper length with a 25-ton press and fixed in length with long thru-bolts in the stacking fixture. Steel plates, 1.91 cm thick, were welded to the top, bottom, and side indentations. Finally, the epoxy between laminations was cured at 300°C for five hours. Laminations are glued together except that the end packs are removable and bolted to the back packs.

The coil consists of four pancakes, each having 10 turns of 1.588-cm x 4.445-cm copper conductor. Electrical leads, water leads, and jumpers connect to the coils at the outside center of the dipole. The coils can be tilted at an angle to the pole face as a quadrupole adjustment to the field. Figure 4 is a photograph of the assembled magnet.

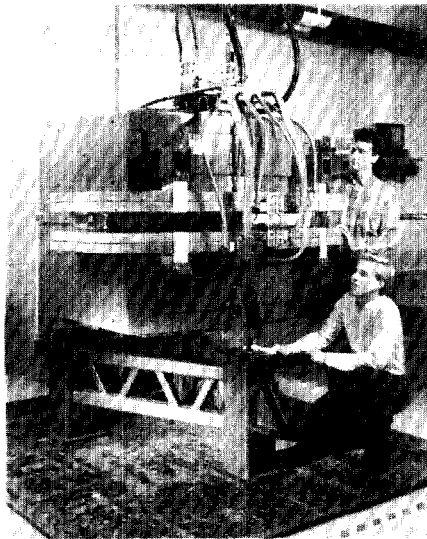


Figure 4: Assembled Prototype Dipole

### Field Mapping System

A system was designed and constructed to map the magnetic field of the dipoles and other magnetic

elements including solenoids and toroids of a proposed Electron Beam Cooler. The field sensing device is a temperature-compensated Hall-effect probe. Positioning of the probe within the field area is accomplished by a personal computer (PC) based, x-y positioning system.

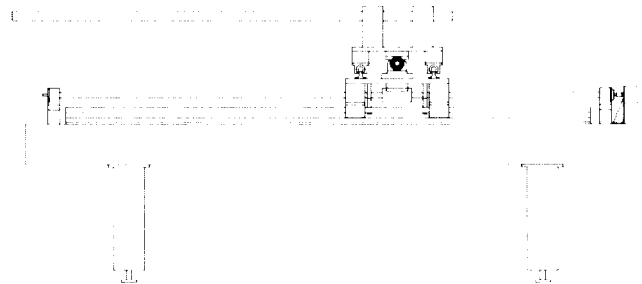


Figure 5: Magnetic Field Mapping Structure

The mapping structure shown in Fig. 5 is built on a 1.22 x 3.05 m, nonmagnetic, stainless-steel laser table. Two case-hardened and ground bearing shafts are mounted along the 3.05-meter dimension at a separation distance of 111.13 cm. Twin ball-bearing bushings are mounted on each rail and spanned by an aluminum bridge assembly to yield one degree of motion. Similarly, two shafts and associated bearings are mounted along the bridge, spanned by an aluminum plate, to yield the second degree of motion. Two slide and vise assemblies are mounted vertically on the top bridge to hold a horizontal boom to position the Hall probe in the dipole gap. This 3.05-m, cantilevered boom was constructed using lightweight honeycomb paper wrapped with resin-impregnated, graphite tape. Horizontal motion is obtained by driving ball screws with stepping motors. Travel in the horizontal plane is limited to 215.9 by 88.9 cm, and the maximum manual vertical adjustment is 15.24 cm.

The control and data acquisition system is shown in Fig. 6. A stepper motor controller board mounted in the PC controls the initial and maximum stepping rates, acceleration rate, stepping direction, and number of steps for two motors. Step-to-pulse translator/driver/power supply units interface the PC board and motors. Each step corresponds to a 1.8° rotation of the motor shaft. Motors are coupled to the ball screws using timing belts to damp out vibrations.

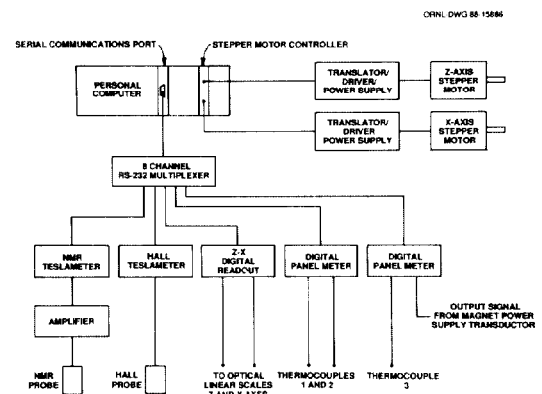


Figure 6: Control and Data Acquisition System for the Magnetic Field Mapping Structure

Optical linear scales of 0.01-mm resolution are mounted along each horizontal axis to provide position feedback via a digital readout box. The Hall probe contains a thermal sensor and is connected to a Teslameter which compensates for temperature fluctuations. An NMR probe is mounted in the dipole center for calibration checks of the Hall probe at regular

intervals during mapping. Three thermocouples connected to digital panel meters are used to provide coil, yoke, and ambient temperature measurements. Each of the above devices provides output through an RS-232C serial interface.

During the mapping process, horizontal motion is controlled by a compiled BASIC program which programs stepping motor controller integrated circuits on the PC board for specified motion patterns. The software also reads information from the RS-232C devices, displays it, records relative extrema, and writes the information to a floppy disk for later data reduction.

### Field Measurements

The midplane of the prototype dipole has been mapped over its entire magnetic field range. A given mapping consists of 419 points along each of 21 curved, parallel orbits, each orbit separated by 1 cm. Mapping points are located along an orbit such that the path length between points is constant at 5 mm, yielding a total path length of 209 cm. This approach yields simplified field calculations. Positioning accuracy along a single axis is assured to within 0.04 mm for each of the 8799 mapping points.

The dipole field was mapped at 15 excitation levels ranging from 72 to 2406 A, or 0.06 to 1.61 T. Figure 7 shows representative middle and high field profiles. Each plot shows field profiles in the central region of the dipole (triangles) and profiles integrated along the ion path length (squares connected by line). These measurements show a small quadrupole component in both the central and integrated profiles. This quadrupole component was not predicted by either TOSCA or POISSON and also appears in the IUCF<sup>5</sup> and Heidelberg<sup>6</sup> dipoles. The origin of this difference is not understood. However, this quadrupole component can be compensated, if needed, by adjusting the main quadrupole strengths, fabricating pole face windings, or making small geometrical changes in the lattice. The measured sextupole and octupole components of the field are small, and consistent with the magnet code predictions. With decreasing excitation, the quadrupole component decreases and changes sign. This decrease is consistent with a remnant field measurement of 30 G with a  $\pm 2$  G quadrupole component at  $\pm 6$  cm.

The integrated curves of each of the 15 mappings were approximated with a least-squares fit for a polynomial of the form

$$\frac{B(x) - B_0}{B_0} = \frac{B'x}{B_0} + \frac{B''x^2}{2B_0} + \frac{B'''x^3}{6B_0}$$

where  $x$  is the equilibrium orbit deviation in meters. Table 1 gives the quadrupole,  $B'/B_0$ ; sextupole,  $B''/2B_0$ ; and octupole,  $B'''/6B_0$  components of the dipole.

Table 1: Multipole Coefficients of the Dipole

Amps	Field Gauss	L-eff m	B'/B <sub>0</sub> 1/m	B''/2B <sub>0</sub> 1/m <sup>2</sup>	B'''/6B <sub>0</sub> 1/m <sup>3</sup>
72	607	1.2793	0.0186	-0.0304	1.4241
125	863	1.2839	-0.0068	0.0284	1.3788
230	1587	1.2932	-0.0131	-0.0150	1.6267
327	2269	1.2967	-0.0224	-0.0160	1.8956
555	3887	1.2981	-0.0257	-0.0103	2.0764
704	4970	1.2983	-0.0241	-0.0126	1.8866
906	6380	1.2997	-0.0238	-0.0062	1.9210
1130	7959	1.2984	-0.0223	-0.0061	1.9090
1312	9249	1.2987	-0.0209	-0.0052	1.9218
1519	10650	1.2984	-0.0201	-0.0071	1.9669
1729	12181	1.2993	-0.0184	-0.0303	1.9597
1936	13537	1.2982	-0.0180	-0.0202	2.0052
2134	14800	1.2961	-0.0177	-0.0766	2.1009
2343	15827	1.2941	-0.0186	-0.1627	2.1994
2406	16111	1.2942	-0.0186	-0.1821	2.0858

Knowing these coefficients permits physical magnetic elements in the ring to be tuned for proper beam focusing. Tracking studies of the HISTRAP lattice are being performed with these multipole components in the dipole magnets. Correction magnets for the octupole component may not be required. The magnet's effective ion path length is also tabulated.

### Summary

A prototype dipole has been successfully designed, constructed, and mapped. Results showing almost identical integrated and central profiles verified that the curved and angled coil end design did cancel the sextupole component found in typical C-shaped dipoles with straight coil ends. Except for the small quadrupole component, the predicted field profiles very accurately modelled the actual field profiles. This includes the predicted loss of field shape at both high and low excitation. The prototype dipole is adequate and will be used without modification for HISTRAP construction.

### References

1. D.K. Olsen et. al., Nucl. Instrum. Methods Phys. Res. B24/25, p.26 (1987).
2. S.W. Mosko, D.T. Dowling, D.K. Olsen, "Prototype RF Cavity for the HISTRAP Accelerator," paper D37 of this conference.
3. J.W. Johnson et. al., "HISTRAP Vacuum Test Stand for Pressures of 10<sup>-12</sup> Torr," American Vacuum Society 35th National Symposium and Topical Conference, Atlanta, October 1988.
4. F. Cole, et. al., IEEE 87CH2387-9, p.1985 (1987).
5. T. Sloan, O. Dermois, and M. Yurko, IEEE 87CH2387-9, p.1443 (1987).
6. D. Kramer et. al., "The Magnet System of TSR," EPAC, Rome, June 1988.

906 A. 6380 Gauss

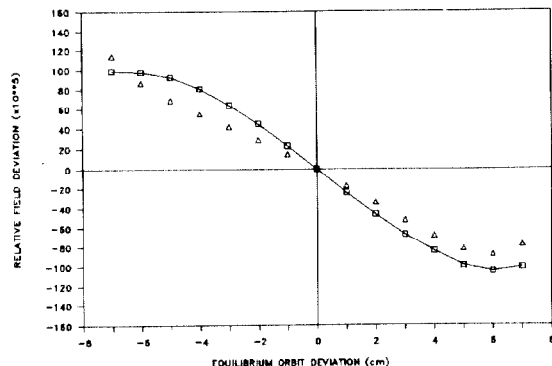


Figure 7: Measured Field Profiles

$dB/B \times 10^{**5}$  vs. distance from equilibrium orbit (cm)

2343 A. 15,827 Gauss

